UNIVERSITY OF MINNESOTA
Driven to Discover℠

Suite 1000 ME
111 Church St. SE
Minneapolis, MN 55455-0111

Project Title: Embedded Nanocrystal Silicon Films: A New Paradigm for Improving the Stability of Thin-film Silicon

Contract Number: RD-3-25 **Milestone Number:** 8 **Report Date:** 6 Dec 2010

Principal Investigator: Uwe Kortshagen
612-625-4028

Contract Contact: Amy Rollinger
612-625-1359

Congressional District: (Corporate office) Minnesota 5th

Congressional District: (Project location) Minnesota 5th

MILESTONE REPORT

Executive Summary:

Under this grant, we pursue two different routes that may help increase the efficiency and lower the cost of thin film silicon solar cells. Our first approach (***Track 1***) is based on our unique ability to produce silicon nanocrystals in a low-pressure plasma-based synthesis reactor and to embed these nanocrystals in amorphous silicon films. Our novel deposition process enables us to independently control the properties of the amorphous matrix and of the crystalline phase, which we hope will enable us to improve the electronic quality of amorphous silicon that is used in thin film solar cells. In the second approach (***Track 2***), we study using such embedded nanocrystals as nuclei for seed-induced re-crystallization of amorphous silicon films. We expect that controlling the seed concentration will enable us to grow microcrystalline Si films faster and with grain sizes larger than possible with other deposition approaches. This may enable the cheaper production of solar cells based on microcrystalline silicon.

During the current project period, efforts under track 1 have focused on understanding the role of embedded nanocrystals on the hydrogen motion in amorphous silicon films. We observed that embedded silicon nanocrystals seem to impede the motion of hydrogen in the amorphous silicon films. We believe that this impediment to hydrogen transport may play an important role in the improved stability of amorphous silicon films with nanocrystal inclusions.

In track 2 studies focused on investigating the role of strain of the films on the crystallization kinetics. Strain in the films was studied with Raman spectroscopy. We observed that the incorporation of silicon nanocrystals leads to strong enhancement of the initial tensile strain of the seeded films, which likely contributes to the fast crystallization of the films. After the onset of crystallization, strain is rapidly reduced and it reaches a saturation value when crystallization reaches its maximum.

Project funding provided by customers of Xcel Energy through a grant from the Renewable Development Fund.

Technical Progress:

Both tracks of the project have made good progress and achieved the milestone set in the contract. The progress made on both tracks will be discussed below.

Track 1: ***Embedded nanocrystals in amorphous silicon***

Within this research track, we are continuing to study the effects of the embedded silicon nanocrystals on the optical and electronic properties of hydrogenated amorphous silicon (a/nc-Si:H). This quarter we have examined the relationship between hydrogen motion (known to occur in hydrogenated amorphous silicon (a-Si:H)) and the electronic properties of the mixed-phase a/nc-Si:H. Hydrogen bonding and motion has been linked to the formation and stability of light induced defects in a-Si:H, known as the Staebler-Wronski effect (SWE), a phenomenon that limits the efficiency of a-Si:H based photovoltaic devices. Consequently an understanding of the influence of silicon nanocrystallite inclusions on the hydrogen motion and bonding structure may help elucidate the reason for the enhanced resistance of a/nc-Si:H films to the SWE. As described in the first quarterly report (Q1), a dual plasma system has been used to produce silicon nanocrystals in one plasma deposition system. The particles generated in this system are then entrained by a carrier gas and injected into a second plasma deposition system. These nanocrystals are embedded into a hydrogenated amorphous silicon film being grown in the second plasma chamber.

Bonded hydrogen within an a-Si:H film is highly mobile and the sub-network which the hydrogen forms has properties not unlike a glass, which affect the electronic properties of the film [1, 2]. These are often collectively referred to as "thermal equilibrium" effects, as they resemble a glass in its out-of-equilibrium state. At temperatures below the equilibrium temperature (T_E), typically around 130°C for n-type doped a-Si:H, the film is actually in a metastable state, with a thermal-history dependent conductivity and isothermal stretched exponential relaxation behavior. While these phenomena have been studied in great detail in doped a-Si:H, the question of how nanocrystalline inclusions affect the glass-like properties of the amorphous matrix within which they reside has not been explored.

As before, the crystal fraction was determined via Raman spectroscopy; n-type doped a/nc-Si:H films with crystal fractions (X_C) of 0, 19, 25 and 29% have been studied to date. The data was acquired using the same equipment and settings as in reference [3]. The thermal equilibration properties were studied using the conductivity measured as a function of temperature for different thermal treatments. Briefly, the samples are taken to 470K, allowed to reach equilibrium (where the conductivity is no longer time-dependent) and then quenched to 320K at varying rates, from 0.1 K/min to 100 K/min. The conductivity of the film is then measured upon warming at a constant rate of 2-3 K/min. This process was repeated for all four films. To further analyze the data, a temperature-dependent activation energy can be defined for the conductivity data. When the conductivity has the form:

$$\sigma = \sigma_0 \exp[-\beta E_A(T)] \quad (1)$$

where $\beta = 1/k_B T$, the activation energy, $E_A(T)$, can be calculated using a simple derivative:

$$E_A(T) = -\frac{d \ln \sigma}{d\beta} \quad (2)$$

This analysis is inspired by Hill [4] and Zabrodskii [5]. When the activation energy is plotted as a function of temperature, a shift in the activation energy is expected at the transition between the metastable and in equilibrium regimes of the hydrogen glass.

An example of a typical measurement for doped a-Si:H without nanocrystalline inclusions is shown in figure 1. For temperatures below a certain temperature labeled T_E, the curves for differing quench rates merge together and are independent of thermal history. The inset shows a plot of the activation energy, calculated per equation (2), which clearly shows the transition from a low-temperature activation energy to a higher value above T_E. The activation energy analysis is particularly useful for defining T_E. We show this analysis for all the films at one cooling rate (1 K/min) and define T_E as the start of the transition between activation energies. This is shown in figure 2a as the intersection of the two straight lines fitting the data. The resulting thermal equilibration temperatures have been plotted as a function of crystal fraction in figure 2b. As can be clearly seen, T_E increases with increasing crystal fraction. This increase in T_E with increasing X_C can be tentatively interpreted as a slowing of the hydrogen motion, due to a decrease in the diffusion coefficient, as a result of the inclusion of the nanocrystallites. This result may help elucidate the mechanism responsible for the reduction in light induced defects in these mixed-phase materials. Clearly, further study of this effect is warranted and will be presented in the next report.

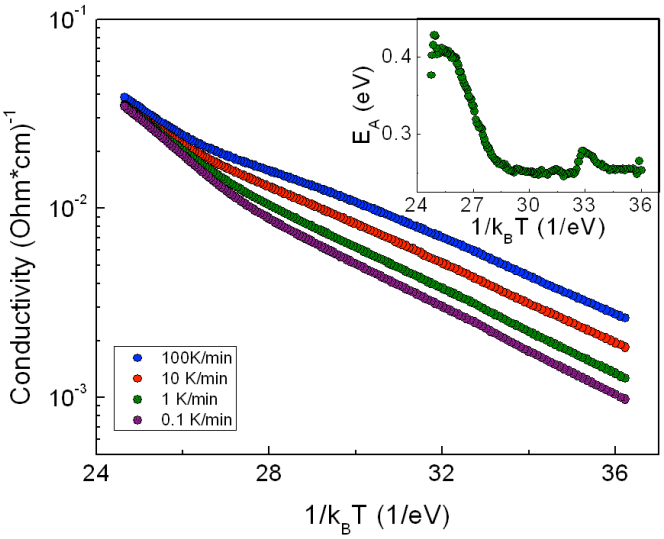

Figure 1: Conductivity for a doped film without nanocrystals, showing the typical transition between metastable and in equilibrium behavior by the shift in activation energy and merging of the conductivity curves from different thermal treatments.

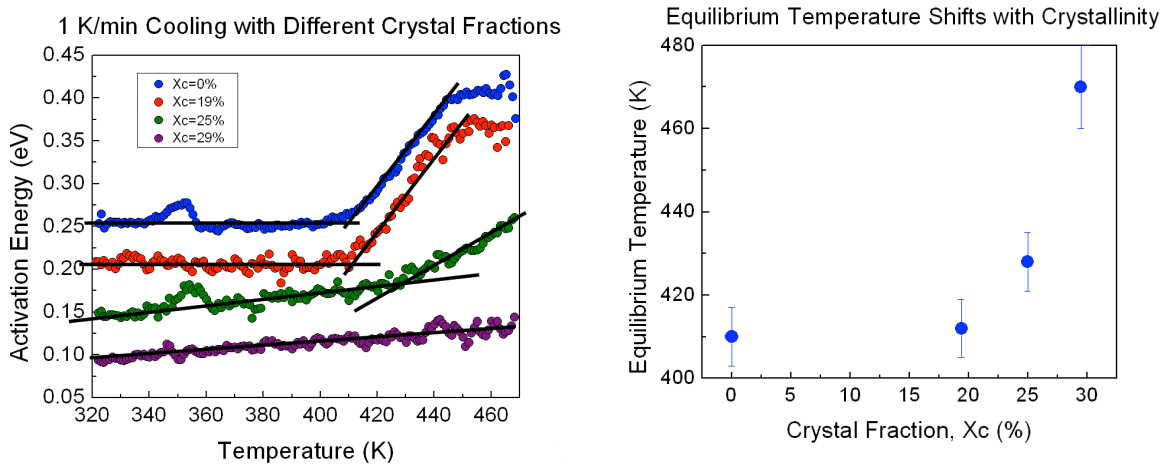

Figure 2a and b: (a) The activation energy as a function of temperature; T_E is being defined as the start of the transition between the two activation energies. (b) The resultant T_E is plotted as a function of crystal fraction.

Track 2: ***Large-grain re-crystallized Si***

The second track of the project aims at controlling the grain structure of micro-crystalline films through the annealing of amorphous silicon films in which silicon nano-crystals are embedded as "seeds" for crystal grain growth. The primary goals for this approach are to reduce the heating (annealing) time required to fully crystallize films as well as to increase the overall grain size within the final crystallized structure, relative to other commonly used processes. Results of quarters past have shown significant success through reduction of required heating times, reproducible control of final grain structure and electronic properties, while also revealing a potentially new mode of solid phase transformation.

Fully exploiting the capabilities of these film structures requires further understanding of this novel mode of crystallization, and a detailed knowledge of the process parameters that affect it. In quarter 7, efforts were focused primarily on macro-scale science of the crystallization process through an investigation of secondary trends suggesting "seed competition based" growth behavior as well as a more in-depth and quantitative characterization of the film stress-state induced by seeding. The efforts of quarter 8 continued with quantitative analysis of the stress state induced by seed inclusion by measuring the variation of stress with particle density.

Numerous studies within the literature have shown conclusively that stresses within the film can significantly influence the crystallization time of amorphous films [6, 7]. Specifically, it has been shown that tensile stress states serve to reduce crystallization time. This is because, unlike metallic thin films, semiconductors are weak in tension [8], and thus lattice expansion weakens bonds and leads to increased atom mobility, allowing for easier diffusion to lower potential arrangements (i.e. across a-Si:H/c-Si interfaces) during crystal growth. Conversely, compressive stresses have been shown to have an opposite effect, causing bonds to become more stable and thus increasing the required energy needed to mobilize atoms for grain growth [9-11].

Previous quarters' measurements studied the variation of stress with anneal time of samples having equivalent seed populations. The results of these studies showed each sample to exhibit dramatically different stress states than those commonly found in amorphous (unseeded)

films in the literature. For instance, pure amorphous silicon (without any crystalline phase present) is known to have an as-deposited stress state that is controlled by hydrogen content and film disorder. Since these two parameters are difficult to de-couple from one another in most film deposition methods (i.e. increasing Hydrogen content typically also increases film disorder), the precise role of Hydrogen in determining the films stress state is still an issue of contention. Specifically, an increase in film disorder tends to promote tensile stress fields while an increase in hydrogen content is argued to be able to induce both tensile and compressive stress depending on its configuration and the method of incorporation within the film. For films deposited in manners similar to ours, by PECVD, hydrogen concentrations are relatively large compared to other methods.

Most literature studies involving a-Si:H synthesized in this manner are reported as having compressive stress states, as-deposited. However separate reports have shown that additional hydrogen is capable of both increasing this compressive stress and reducing it. Despite these contradictions, most studies typically show that, upon annealing, the initially compressive stress state of the film is gradually relieved, increasing toward zero during the film incubation period. Once native nucleation begins, the transformation of numerous points within the film to a denser, crystalline phase causes points of contraction which pull on their less dense, amorphous surroundings, thus inducing a gradually increasing state of tension within the film. As the volume percent of the crystalline phase saturates to the final value, the film stress saturates at a final tensile value near around 400MPa.

Our seeded films, however, experience stress states dramatically different from those commonly reported in literature studies. Rather than exhibiting a compressive stress field in their as-deposited state, we showed in quarter 7 that seeded films display extremely large tensile stresses; much larger than those predicted by thermal expansion coefficient mismatches between film and substrate. Upon annealing, these stresses decrease as the film progresses towards complete crystallization, interestingly arriving at a final saturation tensile stress near 400-600MPa.

Since all of the films involved in the quarter 7 study consisted of equivalent seed structures, in order to determine if this tension was inherent to our amorphous film deposition or directly linked to the seed inclusions, in quarter 8 we deposited several films of varying initial seed densities, including an unseeded control film and performed a parallel experiment. Furthermore, a different method of stress measurement was implemented, in order to provide verification that the values seen previously were not a consequence of a bias within the characterization technique.

Subsequently, the stress values of each film were measured using Raman spectrometry in resonance with the silicon direct band gap [12], where a spatial resolution of less than 1μm can be obtained. Compared to the Profilometer probes used in quarter 7, Raman measurements have certain advantages. For instance, Raman frequency shifts, caused by residual stress in the silicon film are usually very small, with a Raman shift of about $0.08cm^{-1}$ typically corresponding to a 40MPa stress variation [13], thus providing a more sensitive measurement. Also Raman has better spatial resolution on the micrometer scale, which helps to minimize the effect of substrate interfacial effects and thermal stress effects. The relationship between mechanical stress and the shift of the Raman transverse optical (TO) peak shift is given by:

$$\sigma(\mathrm{Mpa}) = -250\Delta\omega(\mathrm{cm}^{-1}),$$

where $\Delta\omega = \omega_s - \omega_0$. ω_0 is the wave number of the stress free single crystal (520.5cm^{-1}) and ω_s is the center position of the Gaussian peak corresponding to the TO phonon mode in amorphous silicon. A peak shift towards lower wave numbers indicates tensile stress, and a shift towards higher wave numbers is related to compressive stress. Raman spectra were recorded for five samples of varying initial seed concentration along with a sixth, unseeded sample, in the as-deposited state as well as throughout a complete annealing process carried out at 650C. As seen in figure 3, the as-deposited stress states of the films show all samples, seeded and unseeded, to exhibit a tensile stress state as-grown. Furthermore, the trend shows a sharp stress increase with even a small number of seed inclusions, which increases further with the addition of more seeds. This seems to indicate that, although the non-conventional tensile stress state is not caused solely by the seed inclusions, it does seem to be enhanced by their presence.

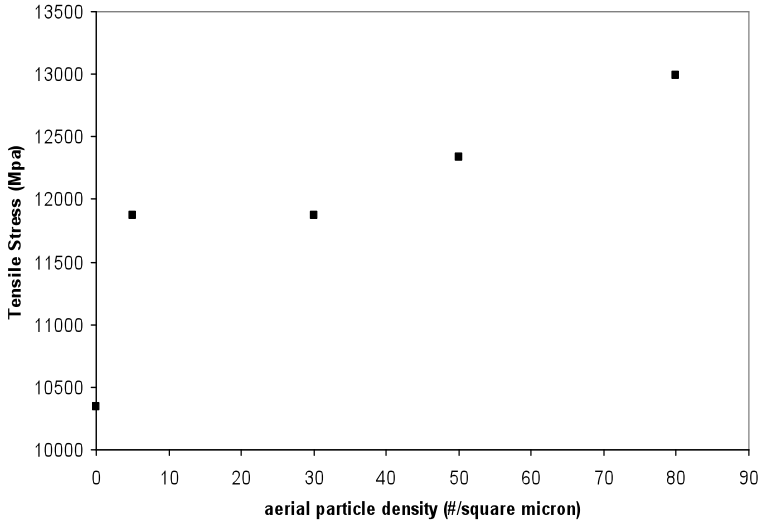

***Figure 3**: Plots of residual stress vs. aerial density of embedded seed crystals, for films having 5 different seed densities. The sample intersecting the y-axis corresponds to an unseeded, control sample.*

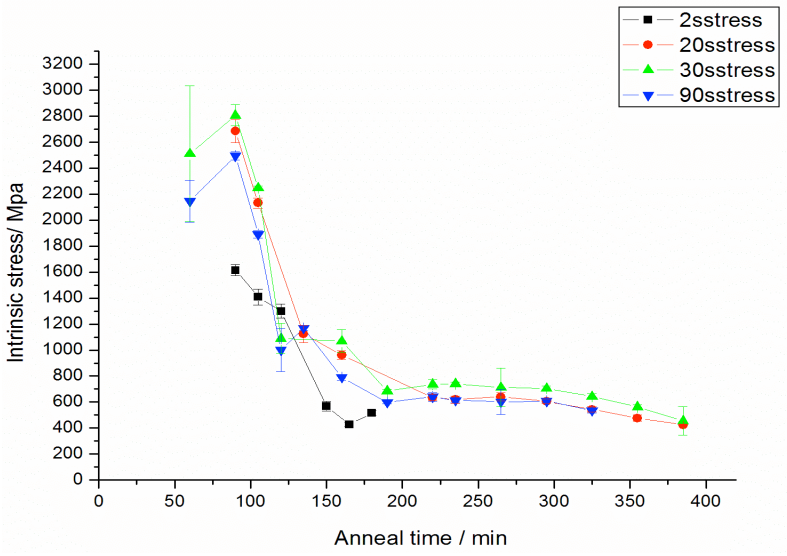

***Figure 4**: Time-series plots of residual stress vs. annealing time for seeded films at different seed density. "2s" and "90s" correspond to the lowest and highest initial seed densities, respectively.*

Figure 2 shows the evolution of the stress of each of the films from figure 3, as they are annealed to full crystallization at 650C. As opposed to most films observed in literature where a compressive stress is seen to become more tensile throughout crystallization, here we see, once again, an initial state of tension decreasing toward lower values. Although there is no clearly evidenced trend between seed density and rate of stress decrease, it is interesting to note that the stresses for two of the seeded samples appear to rise momentarily in the initial stages of the annealing process, before falling dramatically. Since it has been seen in literature that molecular hydrogen filled voids area capable of producing large pressures (on the order of 200MPa or more) [14], this may be a stress signature of the void formation discussed in quarter 3. Although it is not yet concluded whether the voids are filled with hydrogen, it is interesting to note that the time interval over which the stress increases corresponds to the time between when voids were observed to reach full size and begin propagating through the film. Furthermore, the time at which stress values for each film begin to saturate is approximately the same time at which crystal fraction values begin to saturate. This suggests a clear link between the crystallization process and the stress state within the film, however further studies over smaller time windows and larger seed density variations will have to be conducted to gain a clearer understanding of the precise role of stress on the seeded grain growth kinetics, as it may vary with seed density.

Additional Milestones: Work is in progress towards milestone 9.

Project Status: The project is on schedule. A journal publication is currently being worked on and submission is expected during quarter 9. Two conference presentations were submitted during quarter 7 (see appendix to milestone 7 report) and presented during quarter 8.

Milestone 8

To be completed 24 months after the Contract Start Date

Track 1: Embedded nanocrystal amorphous Si – Complete establishment of main parameters affecting optical and electronic properties of the embedded nanocrystal amorphous films. Complete determining effect of amorphous matrix deposition conditions on film properties for given nanocrystal size and density.

Track 2: Large-grain recrystallized Si - Continue to establish main parameters affecting the crystal growth kinetics, incubation time, and grain size distribution. Continue to study influence of hydrogen-content of amorphous matrix on recrystallization.

Deliverable 8:

Provide 1 x 2 cm^2 film sample. A journal publication (submitted) and conference presentation. Submission of Milestone Report detailing completion of Milestone 8 requirements to RDF representative.

References:

1 J. Kakalios and W. B. Jackson, "The Hydrogen Glass Model", edited by H. Fritzsche (*World Scientific Publishing Company*, 1988), p. 207

2 J. Kakalios and R. A. Street, "Thermal Equilibrium Effects in Doped Hydrogenated Amorphous Silicon", edited by H. Fritzsche (*World Scientific Publishing Company*, 1988), p. 165

3 Y. Adjallah, C. Anderson, U. Kortshagen, and J. Kakalios, "Structural and electronic properties of dual plasma codeposited mixed-phase amorphous/nanocrystalline thin films", *J. Appl. Physics* **107**, 043704 (2010)

4 R. M. Hill, "On the observation of variable range hopping", *Phys. Stat. Sol.* (A) **35**, K29 (1976)

5 A. G. Zabrodskii, "Hopping conduction and density of localized states near the Fermi level", *Sov. Phys. Semicond.* 11, 345 (1977)

6 J. Park, S. Kwon, S.I. Jun, I. N. Ivanov, J. Cao, J. L. Musfeldt d, P. D. Rack 2009, "Stress induced crystallization of hydrogenated amorphous silicon", *Thin Solid Films*, **517** 3222–3226.

7 M. Hossain, H. Naseem, and W.D. Brown 2006, "Effect of stress on the aluminum-induced crystallization of hydrogenated amorphous silicon films", *J. Mater. Res.*, **21**(10) p. 2582-2586.

8 Ohring, Milton. "Materials Science of Thin Films: deposition and structure, second edition", *Academic Press*, 2002.

9 P. Hashemi, J. Derakhshandeh, and S. Mohajerzadeh, M. Robertson and A. Tonita 2004, "Stress-assisted nickel-induced crystallization of silicon on glass", *J. Vac. Sci Technol. A*. **22**(3)

10 M. Moniwa, M. Mlyao, R. Tsuchiyama, A. Ishizaka, M. Ichikawa, H. Sunami, and T. Tokuyama 1985, "Preferential nucleation along Si02 steps in amorphous Si", *Appl. Phys. Lett.* **47**(2) p. 113-115.

11 Y. Kimura, M. Kishi and T. Katoda 1999, "Effects of elastic stress introduced by a silicon nitride cap on solid-phase crystallization of amorphous silicon", *J. Appl. Phys.* **86**(4*)* p. 2278-2281.

12 Thanh Nga Nguyen, V.D.N., Sungwook Jung, Junsin Yi 2009, "Raman scattering analysis of the residual stress in metal-induced crystallized amorphous silicon thin films using nickel"*, Applied Surface Science*. **255**(19) p. 8252-8256.

13 Wolf, I.D. 1996, "Micro-Raman spectroscopy to study local mechanical stress in silicon integrated circuits"*, Semiconductor Science and Technology*. **11**(2) p. 135-154.

14 J. B. Boyce, M. Stutzman, S. E. Ready 1985, "Molecular hydrogen in amorphous Si: NMR studies"*, J. Non-Cryst. Solids*. **77-78**(1) p. 265-269.